LABORATORY TEST PREDICTIONS OF THE CYCLIC AXIAL RESISTANCE OF A PILE DRIVEN IN NORTH SEA SOILS

MJ Rattley
Fugro GB Marine Limited, Wallingford, UK

L Costa
Scottish Power Renewables, London, UK

RJ Jardine
Imperial College, London, UK

W Cleverly
Offshore Wind Consultants Limited, London, UK

Abstract
Current international guidance recommends that cyclic loading effects are considered in pile design. However, methods for quantifying these effects on axial capacity are not well developed. Simplified methods exist, including generalised interaction diagrams, but they may not be able to address site-specific aspects of soil behaviour, layering, pile geometries or cyclic loads. Applying 'one size fits all' cyclic loading factors is likely to be either inappropriate or uneconomic in wind farm applications, where turbines may be spaced kilometres apart with geology and water depth varying between positions. This paper describes how carefully controlled laboratory tests on site-specific soils allowed case-by-case cyclic analyses to be developed for a major wind farm site in the North Sea. Interpretation of cyclic laboratory tests on sand and clay, within an effective stress framework, allowed the potential cyclic degradation of pile shaft friction to be assessed. The practical approach outlined is shown to provide a feasible route to assessing turbine-specific cyclic factors for offshore pile design.

1. Introduction

1.1 Background

Assessing how cyclic loading affects offshore jacket foundation piles may be more important than previously appreciated, particularly for structures where the cyclic axial pile load component is significantly higher than the static (average) load (Jardine et al., 2012). International standards, such as API (2011) recommend allowing for cyclic effects, but this is often assumed to be implicit in the static methodologies and factors of safety applied under storm loading conditions. The recent drive for increased foundation design efficiency in large offshore wind farm (OWF) developments has prompted a rise in practitioners' use of modern design methods, such as the Imperial College Pile (ICP) method (Jardine et al., 2005). Such methods provide a more robust, physically reasonable approach to static axial capacity. However, cyclic loading needs also to be considered explicitly by the designer. Jardine et al. (2005) suggest how this may be approached; this paper addresses the details of practical application for a major OWF project.

1.2 Design Approaches

In ultimate limit state (ULS) axial pile design, the cyclic loading focus primarily concerns quantifying the degradation of pile resistance. A range of methods for estimating this effect is available in the literature, but no standardised application method exists in practice. One widely adopted approach applied for screening purposes involves the use of simple interaction diagrams, which relate the cyclic capacity of the pile to the static capacity. Figure 1 shows one such example, as presented by Jardine and Standing (2012) for steel tubular piles driven in dense sand at Dunkirk, N France. EA-Pfähle (2014) present a similar cyclic design approach, based on the interaction diagram proposed by Kirsch et al. (2011), which is applied routinely in German OWF projects.

Interaction diagrams afford simple screening tools that rely on compatibility between the soil conditions for which the charts were prepared and those at the design location. Precise matches are unlikely at most offshore sites. Key, site-specific, characteristics of cyclic soil behaviour, layering, pile geometries or cyclic loads are therefore likely to be overlooked. Applying single 'one size fits all' interaction charts is likely to be either inappropriate or uneconomic when initial screening indicates a need for detailed cyclic design, especially with offshore wind turbine jackets that may be spaced kilometres apart, with geology and water depth varying between posi-

tions. Approaches for more advanced local soil-pile analysis are outlined by Jardine et al. (2012) and advocated for pile design in carbonate soils by Erbrich et al. (2010). Such analysis is most pertinent when concerns arise with regard to i) potentially brittle soil response and progressive pile failure, and ii) sites with highly variable, or strongly contrasting, soil layering.

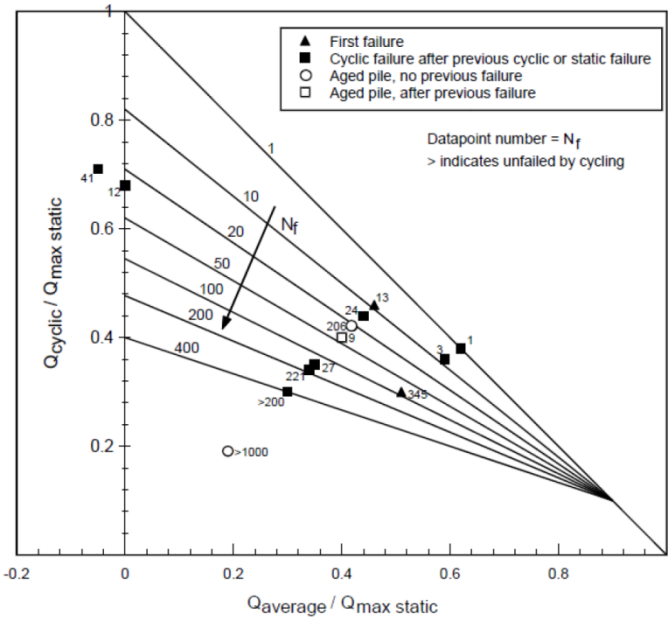

Figure 1: Interaction diagram from cyclic testing of piles driven in dense sand at Dunkirk (Jardine and Standing, 2012)

One route to developing local shaft degradation laws is to conduct cyclic laboratory testing on site-specific soils. This approach provides data on the element level response of the soils which can be used to analyse either global pile degradation or local soil-pile response under cyclic loading. The boundary conditions applied in cyclic laboratory testing affect the results and this must be considered carefully. The laboratory testing approach adopted recently for the East Anglia One (EAONE) OWF is reported in this paper.

1.3 Site Summary

EAONE, which is sited in the southern North Sea, involves 102 7MW wind turbine generators (WTG) whose substructures consist of 3-legged jackets founded on driven open-ended piles; water depths range from 38 m to 50 m. The site geology is typical of the region, consisting of Holocene sediments overlying Pleistocene strata that reached their current state though a series of glaciations and comprise predominantly dense sands and high strength clays. The key formations considered are the Yarmouth Roads, Smith's Knoll and Westkapelle formations, combinations of which are present across the whole site. Sand and clay units of the Westkapelle formation were sampled over the expected foundation depths at multiple locations.

1.4 Soil Properties

Tables 1 and 2 summarise some key geotechnical parameters for the soil units considered.

Table 1: Summary of key soil properties for sand soils

Formation	D_r **[%]**	D_{50} **[mm]**	δ_{cv}[°]	q_c **[MPa]**
Yarmouth Roads	90-110	0.17-0.20*	32	20-60
Smith's Knoll	50-70	0.12	28	10-30
Westkapelle	80-90	0.14	31	40-70

*Range includes formation sublayers

Table 2: Summary of key soil properties for clay soils

Formation	**PI [-]**	**YSR**	δ_{ult}[°]	q_c **[MPa]**
Westkapelle	15-20	2-4	20	4-6
Westkapelle	25-30	2-4	13	3-5

2. Cyclic Laboratory Testing

2.1 Testing Programme

Cyclic degradation laws can be formulated using cyclic triaxial (CTXL) (Aghakouchak et al., 2015), cyclic constant normal stiffness (CNS) tests (Erbrich et al., 2011) or cyclic direct simple shear (CSS) laboratory tests. While simple shear tests offer less comprehensive measurements than triaxial tests of the developed stress and strain conditions, they better match the pile kinematic boundary conditions.

Constant volume CSS tests match the constant volume conditions expected during undrained cycling in clays and provide notionally infinite normal stiffness for drained sand cases. However the constant volume condition is applied irrespective of in situ drainage conditions, load frequency, and variations in cyclic load level. Arguably, CNS testing should provide more realistic measurements of changes in normal effective stress during drained shearing, allowing also for soil response outside of the direct shear zone along the pile. However, such tests require an estimation of the mass horizontal stiffness of the soil, a parameter that is pressure-dependent, varies non-linearly with distance from the pile and depends on the pile diameter. CNS values are not easily obtained or estimated but are likely to be very high in dense North Sea sands.

Hollow Cylinder Apparatus offers the best equipment for simple shear testing, as it provides better boundary conditions and full descriptions of the specimens' stress and strain states. But routine CSS tests provide useful practical measurements in which the constant volume condition is obtained by dynam-

ic control. With most commercial CSS apparatus, the controls lead to very high, but finite, normal stiffness.

Over 40 CSS tests were performed across 5 soil units as part of a comprehensive cyclic laboratory testing programme for EAONE. A small number of CTXL tests were performed to provide a benchmark for the measured CSS response. Intact clay CSS specimens were cut at 90° from core samples during trimming. For reconstituted sand, it was not practicable to create test specimens with grain alignments representative of the soil state around the pile after driving. Instead, the sand CSS tests were prepared by moist compaction to a representative 60% < D_r < 95% range. Although not a focus of this paper, it is acknowledged that the method of specimen reconstitution can influence the measured cyclic response.

2.2 Laboratory Test Specification

For both sand and clay test specimens, the normal stress history applied prior to cyclic loading was designed to broadly replicate the horizontal stress history of the in situ soil, allowing for the effect of pile installation on the soil adjacent to the pile shaft.

For clays, this involved consolidating the specimen under a normal stress equal to the estimated maximum horizontal effective stress for the geological history of the clay. The test specimen was then unloaded to a normal stress equal to the estimated in situ radial effective stress. These stress states were calculated based on available in situ and laboratory test data and the specimen depth below seafloor. Lastly the specimen was reconsolidated under a normal stress equal to the expected radial effective stress adjacent to a pile shaft following installation by driving, calculated according to the ICP method.

A similar approach was applied for sand specimens; however, the initial normal stress was calculated to represent the maximum effective radial stress that might be expected to be generated during driving of an open-ended jacket pile. These effective horizontal stresses were calculated according to the ICP method for equalised effective radial stresses at the pile wall, but with the parameter h, which represents the tip depth of the pile relative to the soil depth, fixed to a value of 0.5 m. This approach resulted in equivalent overconsolidation ratio (OCR) values between 2 and 5, depending on specimen depth. The minimum OCR applies to specimens positioned 0.5 m above the pile tip. To model conditions higher up the shaft, specimens were unloaded to a normal stress equal to the effective radial stress acting on a pile wall after equalisation, predicted according to the ICP method. Following Aghakouchak et al. (2015), all CSS tests on sand included a stage of constant stress (drained) cyclic pre-shearing at their final normal stress to replicate the cycling imposed during pile driving; thirty cycles were applied with a cyclic shear stress ratio of 0.25. Creep intervals of at least 24 hours were applied prior to constant volume cyclic shearing.

Stress-controlled 0.1 Hz sinusoidal cyclic loading was applied to each specimen. The target shear stresses τ applied were normalized by an expected static pile interface shear resistance τ_{rzf} and expressed as τ/τ_{rzf}, where τ_{rzf} is defined as that expected on a steel shaft under a radial effective stress σ'_r. Following Jardine et al. (2005), it is expected that the local static shaft resistance is related to the interface angle of friction δ by Equation 1:

$$\tau_{rzf} = \sigma'_{rf} tan\delta \quad (1)$$

where δ is defined as δ_{cv} in sands and (typically) as δ_{ult} in clays, and σ'_{rf} is the radial effective stress acting on the shaft at failure. The dependency of σ'_{rf} will vary for sand and clay soil conditions.

Cyclic stress ratios τ_{cy}/τ_{rzf} were specified to cover a wide range of values. Average stress ratios τ_{av}/τ_{rzf} were varied over a more limited range that matched the generally low static pile head loads associated with the critical WTG jacket storm loading cases considered at EAONE.

Table 3: Summary of CSS testing

BGS Formation	Soil Type	No. Tests	Specimen D_r [%]	Range of σ'_{n0} [kPa]	Range of τ_{cy}/τ_{rzf} [-]	Range of τ_{av}/τ_{rzf} [-]	Range of N_f [-]
Yarmouth Roads	Sand	8	95	50 - 196	0.21 - 0.61	0.10 - 0.20	10 - >1500^
Smith's Knoll	Sand	12	60	81 - 152	0.20 - 0.56	0.10 - 0.20	12 - >1500^
Westkapelle	Sand	14	85	324 - 1004	0.15 - 0.84	0.10 - 0.20	10 - >1500^
	Clay (LP)	3	-	558	0.32 - 0.80	0.32	>1500^
	Clay (HP)	4	-	702	0.45 - 1.10	0.23	67 - >1500^

LP = lower plasticity
HP = higher plasticity
^ = cyclic loading stages were generally ceased at 1500 cycles

For each specimen tested, the application of τ_{cy} led to changes in σ'_n. Slight increases were observed under the lowest cyclic stress ratios and over a limited number of initial cycles at higher cyclic stress ratios in very dense specimens. However, cycling above a limiting τ_{cy} value led to marked σ'_n reductions that grew progressively as cyclic loading continued. Figure 2 presents an example of the evolution of σ'_n for a high level cyclic test performed on a dense sand specimen that led to failure within 25 cycles.

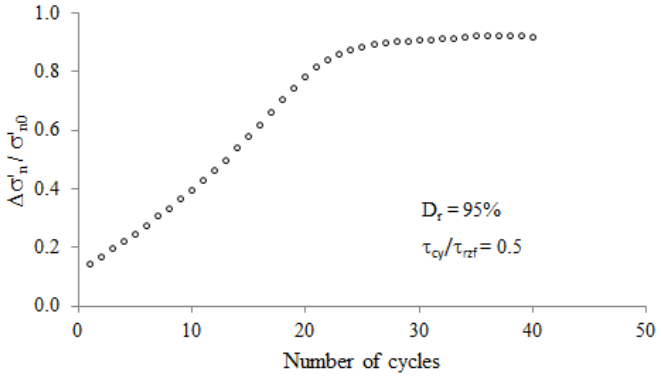

Figure 2: Illustration of normalised reduction in normal effective stress with number of cycles in a CSS test on dense sand

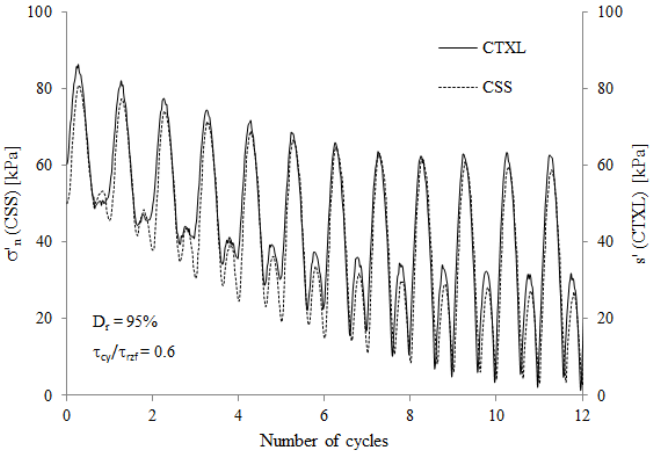

Figure 3: Comparison of variations in two-dimensional normal effective stress from CSS and CTXL tests on very dense sand

CTXL tests were performed to verify the effective stress changes measured in the larger number of CSS tests. Comparison of the data from each test type was generally favourable in the terms plotted in Figure 3, which compares a pair of CTXL and CSS tests performed under similar cyclic stress conditions.

3. Interpretation of Cyclic Test Data

3.1 Interpretation Method

The cyclic design approach should be framed to be theoretically consistent with the static pile design methodology. The OWF considered adopted the ICP (Jardine et al., 2005) in which shaft resistance is controlled by the local radial effective stress during loading and the interface friction angle δ at failure.

Cyclic loading does not influence δ (as defined in Equation 1), which was determined by ring-shear interface tests. The key was then to predict from the cyclic laboratory element tests the reductions in pile shaft radial effective stress expected during storm events. Merritt et al. (2012) and Jardine and Standing (2012) describe one such approach.

The proposed cyclic degradation model aims to first capture the changes in σ'_n measured in the CSS tests. In the interpretation, the σ'_n values on completion of each constant amplitude load cycle are referred to the initial effective stress σ'_{n0} at the start of cyclic loading. Subtracting one from the other gives $\Delta\sigma'_n$ and then dividing by σ'_{n0} allows the proportional loss of effective stress to be quantified. The effective stress reductions grow with the number of applied cycles N for cyclic stress amplitudes above a given 'zero degradation' threshold. As noted earlier, beneficial increases in normal effective stress may be expected below this threshold, although these are not considered further here.

Jardine and Standing (2012) propose that for cycling with τ_{cy}/τ_{rzf} less than $tan\delta$, and for low values of τ_{av}/τ_{rzf} the proportional loss of effective stress is nearly independent of the average shear stress applied. Losses can then be expressed in terms of τ_{cy}/τ_{rzf} and N in the form of Equation 2:

$$\frac{\Delta\sigma'_n}{\sigma'_{n0}} = A\left(B + \frac{\tau_{cy}}{\tau_{rzf}}\right)N^C \qquad (2)$$

where the material coefficients A, B and C define the rate of effective stress reduction under cyclic loading. Jardine and Standing (2012) note that an equivalent $log(N)$ expression may be more appropriate in some soils than the power law given in Equation 2. In addition, although it was adequate for the example case presented, it may not be appropriate in some cases to neglect the average load component and a more complex form of Equation 2 may be necessary.

3.2 Pile-Soil Interface Stability

In the simple shear test arrangement, the samples were prevented from shear at the top and base loading platen interfaces by constraining rings located along the loading platen. Noting that interface shear failure limits the shear stresses that can be sustained by soil positioned at the pile-soil interface, the cyclic

degradation model focuses primarily on the pre-failure CSS test response. Pile shaft failure was defined as the point at which the shear stress ratio (τ/σ'_n) mobilised during the CSS test reached the expected limiting pile-soil interface value ($tan\delta$) for each soil unit.

Higher τ/σ'_n ratios cannot be mobilised close to the pile-soil interface as soil-pile slip initiates when $\tau/\sigma'_v = tan\delta$. Figure 4 illustrates this principle, where the state line corresponding to interface slip given by Equation 1, with the σ'_r for the pile interface being equated to σ'_n in the simple shear test, is plotted in grey.

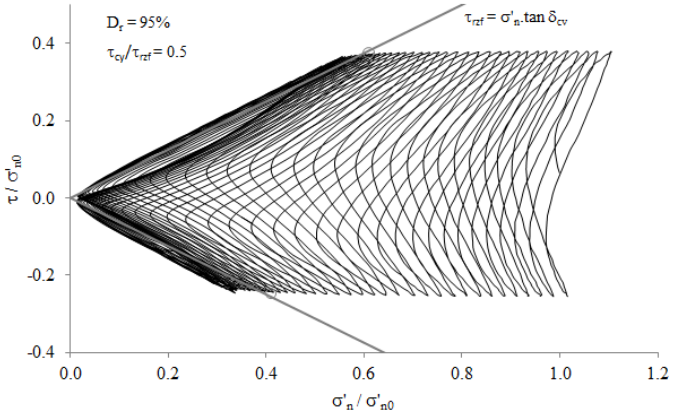

Figure 4: Illustration of test data exclusion outside the limiting stress state

The stress states lying to the left of the state line shown in Figure 4 could not be mobilised by piles in the field as local shaft failure would occur, with each further cycle leading to shear stress transfer to greater depth on the shaft, and hence extra pile displacement.

Jardine et al. (2012) employed cyclic stability diagrams to illustrate the interactive effects on pile capacity of cyclic and mean loads and the number of cycles applied. Their diagrams indicate three distinct phases of pile-soil interface response: a cyclically Stable region, where there is no reduction of load capacity after a large number (say 1000) of cycles , a Metastable phase where some reduction of load capacity occurs after a lower number, N, of cycles, and an Unstable zone where cyclic failure develops within a relatively small number (say 100) of cycles. In the shaft degradation study reported in this paper, all Stable cycles could be eliminated as causing no negative effect. At the other extreme, globally Unstable cyclic conditions were avoided in design as recommended by Jardine et al., (2012). The study therefore focused on modelling the reduction in pile capacity which is accumulated under Metastable conditions, over which significant numbers of cycles may be applied without leading to rapid and unsustainable pile capacity losses.

3.3 Derivation of Model Parameters

Cyclic model parameters were derived from the CSS tests listed in Table 3 to quantify the effective stress changes expected under a range of cyclic conditions. The following degradation parameter is helpful to the discussion below:

$$S = \frac{\Delta\sigma'_n}{\sigma'_{n0}} \quad (3)$$

3.3.1 Sand cases

Figure 5 provides an illustration of the model parameter derivation for Westkapelle sand. Data extracted at the end of load cycles 5 and 200 are plotted against τ_{cy}/τ_{rzf}, covering tests that failed (giving losses of effective stress exceeding 95% of σ'_{n0}) and those where no failure was observed within the maximum number (1500) of cycles imposed. Despite some scatter, a reasonable linear correlation is observed for the two load cycle number cases that support the expression presented in Equation 4:

$$S_{N=i} \approx a\left(\frac{\tau_{cy}}{\tau_{rzf}} - B\right) \quad (4)$$

where a and B are fitting parameters describing the trend gradient and intercept, respectively. The function is subject to limits so that it predicts no change in effective stresses or shaft capacity under cyclic loading with τ_{cy}/τ_{rzf} less than the threshold B.

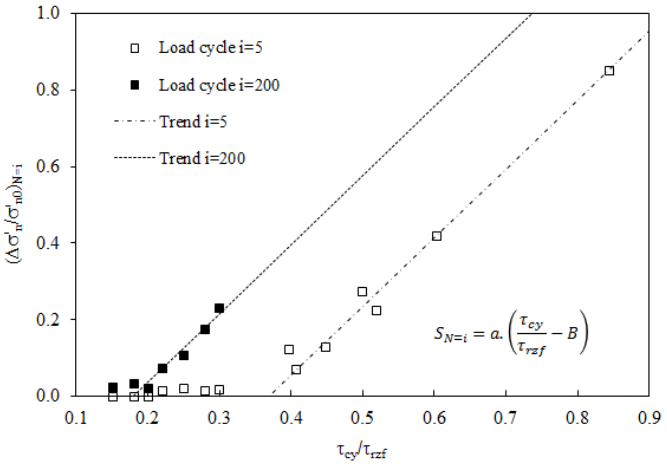

Figure 5: Proportional loss of normal effective stress after 5 and 200 cycles for CSS tests on Westkapelle sand

Overall, Equation 4 fits each set of data plotted well. The experimental deviations fall within the range that could be related simply to the dynamic control

resolution of the test apparatus. However, the trends associated with the N = 5 and N = 200 cases are significantly different. This distinction is linked to the region of response characterising each of the test data points considered. Stable and Metastable tests show no change in normal effective stress over their first five cycles. The N = 5 cases showing significant S values are therefore all Unstable. The fitted trend representing this extreme case would be highly non-conservative when applied to the Metastable area which is of greatest interest in practical design.

In terms of the proposed interpretation, the above observations point to a two-phase response, with a transition point which corresponds to the boundary of the Metastable and Unstable regions. The degradation measured during Unstable load cycling would not be well matched by a Metastable region model of this type and vice versa. This conclusion is consistent with observations by Aghakouchak (2015).

In practical terms, considering the range of average stress ratios represented by the CSS testing, the design of pile sections within the Westkapelle sand formation should aim to keep τ_{cy}/τ_{rzf} below an upper bound of 0.40 to 0.45. In addition, the normalisation process outlined above should focus on the CSS tests that did not fail within 100 cycles and should aim to include cases that showed little or no effect over 1500 or more cycles. It was concluded that the 200 cycle dataset provided a sufficiently conservative basis from which to start the parameter fitting process, as it encompassed an adequate number of tests, including some where cyclic effects were negligible. The same N value was applied to all other soil units.

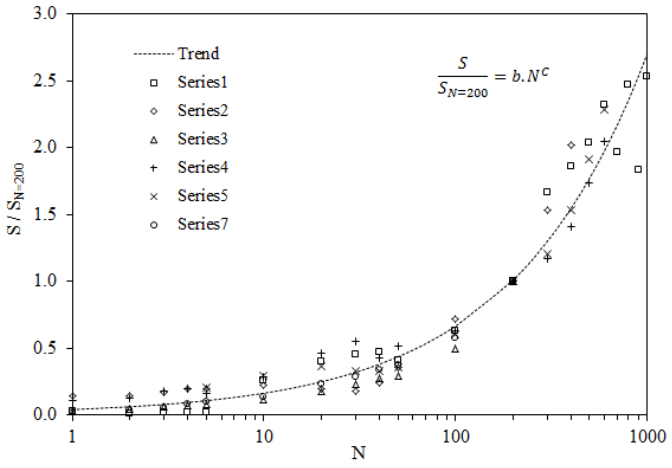

Figure 6: Proportional loss of normal effective stress with number of load cycles for CSS tests on Westkapelle sand

The influence of the number of load cycles is illustrated in Figure 6 where, for each test considered, the value of S at N was divided by the value at N = 200 cycles to demonstrate how the reduction in effective normal stress progresses as cycling continues. A power trend of the form described by Equation 5 provides a reasonable representation of the CSS data shown in Figure 6:

$$\frac{S}{S_{N=200}} \approx bN^C \tag{5}$$

where b and C are fitting parameters which must be adjusted such that the trend passes approximately through 1 at N = 200 and so that the curvature and intercept of the trend provide a reasonable representation of the test data.

Combining Equation 4 and 5 gives Equation 6:

$$S \approx A\left(\frac{\tau_{cy}}{\tau_{rzf}} - B\right)N^C \tag{6}$$

Which is the form proposed by Jardine and Standing (2012) in Equation 2.

3.3.2 Clay cases

The clay units encountered in the Westkapelle formation have varying composition as expressed by both plasticity index (PI) and clay content. These features result in a marked range in the cyclic response seen between the leaner and more plastic sub units. The data presented in Figure 7 are therefore separated into two groups based on PI. For each case, trend lines are drawn for N = 200 cycles.

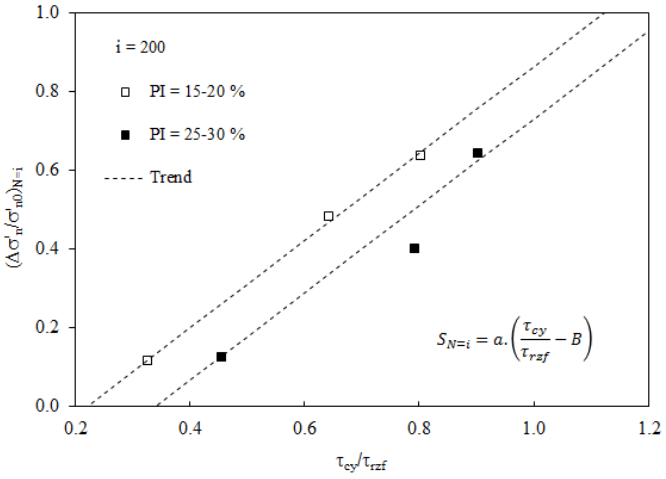

Figure 7: Proportional loss of normal effective stress after 200 cycles for CSS tests on Westkapelle clay

Although only six tests are shown, it is clear that (i) the leaner clay specimens exhibit a significantly lower cyclic damage threshold B and that (ii) the gradients found above the threshold are similar for the two clay compositions.

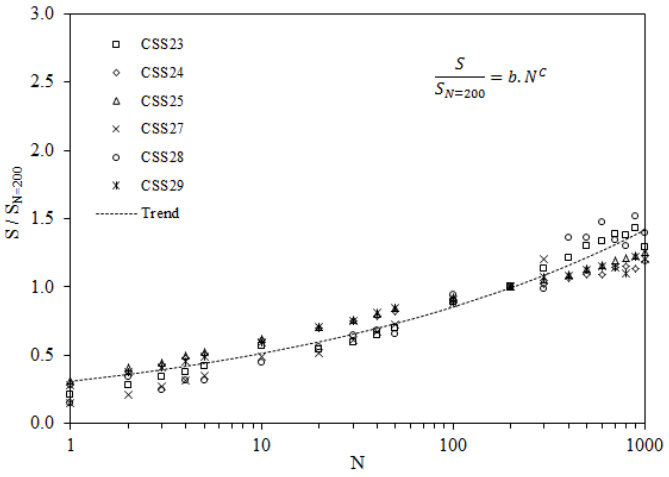

Figure 8: Proportional loss of normal effective stress with number of load cycles for CSS tests on Westkapelle sand

The influence of N on the clays' response is illustrated in Figure 8, where the general trend described by Equation 6 is also plotted. No clear distinction in the proportional loss of σ_n' with N was evident for the different plasticity clays.

3.3.3 Summary of parameters

The cyclic model parameters A, B and C required for Equation 6 were derived for each soil unit based on the testing summarised in Table 3. Table 4 summarises the parameters.

Table 4: Summary of cyclic model parameters

Formation	Soil Type	Model Parameters		
		A	***B***	***C***
Yarmouth Roads	Sand	-0.06	0.19	0.56
Smith's Knoll	Sand	-0.03	0.20	0.64
Westkapelle	Sand	-0.07	0.18	0.61
	Clay (LP)	-0.34	0.22	0.22
	Clay (HP)	-0.34	0.34	0.22

LP = lower plasticity
HP = higher plasticity

Observations include:

- The threshold parameter B increases with plasticity. This is linked to reductions in δ which occur with increasing clay content. Pile interface failure occurs at relatively low proportion of the soil shear strength and the lower δ values effectively shield the soil from cyclic damage;
- Unstable cyclic loading was observed on cycling with τ_{cy}/τ_{rzf} above relatively moderate values (0.40 – 0.45) in sands;
- Proportional loss of effective stress also occurred more rapidly in sands, leading to more marked losses under Metastable conditions and higher C values for sand soil units; and
- Unstable cyclic loading was not observed with the clays tested, even with $\tau_{cy}/\tau_{rzf} > 1.0$. However highly significant losses in effective stress were generated in clays when cycling above the threshold, leading to high A values.

4. Example Pile Prediction

4.1 Calculation Approach

Equation 6 provides a simple tool for predicting the response of the soil under constant amplitude cyclic loading that can be included into local analysis of shaft degradation in layered soil on a pile-by-pile basis. It is, however, easier to illustrate the impact of the model developed from the CSS tests by considering τ_{cy}/τ_{rzf} as broadly analogous to the pile shaft load ratio Q_{cy}/Q_s applied to a pile driven in uniform soil. In this case Q_{cy} is the cyclic load component and Q_s is the pile shaft resistance, and the relative loss of pile shaft resistance can be expressed as a similar function of cyclic load amplitude:

$$\frac{\Delta Q_s}{Q_s} = A\left(\frac{Q_{cy}}{Q_s} - B\right)N^C \qquad (7)$$

Equations 6 and 7 provide a global method of linking the laboratory-measured cyclic response of the soil under constant amplitude cyclic loading to a global pile response. Such a method assumes that pile base loads do not vary during load cycling, and that the cyclic load is distributed over the pile length as a constant proportion of the local shaft capacity. The first assumption may be conservative, while the second may be non-conservative, especially for piles with high length-to-diameter ratios. However, Jardine and Standing (2012) found that the approach applied reasonably well to cyclic tests on piles with 22 < L/D/ 42 driven in dense Dunkirk sand.

Cyclic axial pile forces vary during storm events. The changes in effective radial stress, and therefore shaft resistance, occurring from one packet of applied load cycles to another can be considered using an equivalent number of load cycles. The procedure assumes that the accumulated change in shaft resistance $\Delta Q_s/Q_s$ generated by all previous cycles can be related at the start of each new batch of higher or lower cycles as an equivalent number of cycles N_{eq} applied at the new level of cyclic loading. Merritt et al. (2012) describe the application of such a procedure to the tripod piles that support the Borkum West II OWTG tripod structures.

4.2 Soil Profile

Since cyclic model parameters were derived on a soil unit basis, the distribution of each soil unit at the pile location impacts on the final overall cyclic degradation prediction. For example, based on the de-

rived A, B, C parameters, higher degradation would be predicted at the same value of Q_{cy}/Q_s in the Westkapelle sand unit compared to the Smith's Knoll sand. Piles with a high percentage of their shafts embedded in the Westkapelle sand will therefore suffer greater losses than piles with greater percentages in the Smith's Knoll sand. For the purpose of this example calculation, it was assumed that a pile is installed with equal percentages of shaft area (≈25%) in the Yarmouth Roads, Smith's Knoll formations, and the Westkapelle sand and (high plasticity) clay units.

4.3 Example Calculation

The approach outlined above was applied to estimate the possible reductions in pile shaft capacity due to the axial load cycling expected for the WTG jacket piles for a synthetic 50-year, 3-hour peak storm event and typical pile design dimensions. A peak cyclic load ratio of 0.45 was assumed for this purpose. Table 5 summarises the cyclic degradation calculation for the Westkapelle sand unit.

Table 5: Summary of example cyclic degradation calculation

$Q_{cy}/Q_{cy,max}$	N	Q_{cy}/Q_s	$\Delta Q_s/Q_s$	N_{eq}
0.05	900	0.02	0.00	0
0.17	400	0.08	0.00	0
0.26	200	0.12	0.00	0
0.35	100	0.16	0.00	0
0.45	50	0.20	-0.02	0
0.55	30	0.25	-0.04	8
0.66	15	0.30	-0.06	15
0.77	8	0.35	-0.08	16
0.90	4	0.41	-0.10	15
1.00	1	0.45	-0.10	14

Table 6: Summary of degradation for all soil units

Formation	Soil Type	Cyclic Degradation [%]
Yarmouth Roads	Sand	6
Smith's Knoll	Sand	4
Westkapelle	Sand	10
Westkapelle	Clay	4
	Average [%]	7

Equivalent unit shaft reductions were calculated for the other soil units and the final values are given in Table 6, along with an average percentage reduction in pile shaft capacity. The methodology predicts a significant, but not overwhelming, impact of cyclic loading on axial capacity that could be accommodated in the final foundation design.

5. Conclusions

- No standardised method exists for quantifying the effects of cyclic loading on axial pile capacity;
- Carefully controlled laboratory tests allowed case-by-case, site-specific, cyclic analyses to be developed for the major EAONE wind farm site in the southern North Sea;
- The approach relies on: (i) multiple CSS tests on representative samples of sand and clay and (ii) an effective stress interpretive framework that allows the potential cyclic degradation of pile shaft friction to be assessed systematically;
- Stable, Metastable and Unstable cyclic responses should be carefully distinguished and modelling efforts concentrated on the critical Metastable cases; and
- The approach described offers a feasible and practical means of assessing turbine-specific cyclic degradation design factors that can be accommodated in jacket pile design. This is expected to be particularly attractive for large OWF developments, particularly those subject to future extensions in similar soil conditions.

6. References

Aghakouchak A, Sim WW and Jardine RJ. (2015). Stress-path laboratory tests to characterise the cyclic behaviour of piles driven in sands. *Soils & Foundations.* Vol. 44, No 5, pp 917-928.

Deutsche Gesellschaft fur Geotechnik. (2012). *Empfehlngen des Arbeitskreises 'Pfähle' (EA-Pfähle).* Second Edition. Berlin: Ernst & Sohn.

Erbrich CT, O'Neill MP, Clancy P and Randolph MF. (2010). Axial and Lateral Pile Design in Carbonate Soils. *Frontiers in Offshore Geotechnics, Perth, Australia, November 2010*

Jardine RJ, Chow FC, Overy R and Standing RJ. (2005). *ICP Design Methods for Driven Piles in Sands and Clays*. London: Thomas Telford.

Jardine RJ, Puech A and Andersen KH. (2012). Cyclic Loading of Offshore Piles: Potential Effects and Practical Design. *7th Int. Conf. on Offshore Site Investigation and Geotechnics. SUT, London*, pp 59-100.

Jardine RJ and Standing RJ. (2012). Field axial cyclic loading experiments on piles driven in sand. *Soils and Foundations*, **52** (4), pp 723-736.

Kirsch F, Richter TH and Mittag J. (2011). Zur Verwendung von Interaktionsdiagrammen beim Nachweis Axial-Zyklisch Belasteter Pfähle. *Bautechnik 88*, pp 319-324.

Merritt A, Schroeder F, Jardine, RJ, Stuyts B, Cathie D and Cleverly W. (2012) Development of pile design methodology for an offshore wind farm in the North Sea. *7th Int. Conf. on Offshore Site Investigations and Geotechnics, SUT, London*, pp 439-448.